Biosensors and Bioelectronics 23 (2008) 1759–1768

Contents lists available at ScienceDirect

Biosensors and Bioelectronics

journal homepage: www.elsevier.com/locate/bios

Review

Bond-rupture immunosensors—A review

Evan R. Hirst[a,b,*], Yong J. Yuan[a,b,*], W.L. Xu[b], J.E. Bronlund[b]

[a] Industrial Research Limited, Crown Research Institutes, 69 Gracefield Road, PO Box 31-310, Lower Hutt, New Zealand
[b] School of Engineering and Advanced Technology, Massey University, Private Bag 102 904, Auckland, New Zealand

ARTICLE INFO

Article history:
Received 1 November 2007
Received in revised form 14 January 2008
Accepted 6 February 2008
Available online 13 February 2008

Keywords:
Immunosensor
Bond-rupture
QCM
SAW

ABSTRACT

It has long been the goal of researchers to develop fast and reliable point-of-care alternatives to existing lab-based tests. A viable point-of-care biosensor is fast, reliable, simple, cost-effective, and detects low concentrations of the target analyte. The target of biosensors is biological such as bacteria or virus and as such, the antibody–antigen bond derived from the real immune response is used. Biosensor applications include lab-based tests for the purposes of diagnostics, drug discovery, and research. Additional applications include environmental, food, and agricultural monitoring. The main merits of the bond-rupture method are quick, simple, and capable of discriminating between specific and non-specific interactions. The separation of specific and non-specific bonds is important for working in real-life complex serums such as blood. The bond-rupture technique can provide both qualitative results, the detection of a target, and quantitative results, the concentration of target. Bond-rupture achieves this by a label-free method requiring no pre-processing of the analyte. A piezoelectric transducer such as the quartz crystal microbalance (QCM) shakes the bound particles free from the surface. Other transducers such as Surface Acoustic Wave (SAW) are also considered. The rupture of the bonds is detected as electronic noise. This review article links diverse research areas to build a picture of a field still in development.

Contents

1. Introduction

The analytical applications of quartz crystal microbalance (QCM) are well established and the publications and commercial products that utilise QCM as an immunosensor are too many to name, some examples are (Cooper and Singleton, 2007; Janshoff and Steinem, 2001b; Godber et al., 2005; Huang and Cooper, 2006; Kurosawa et al., 2003). In addition to the popular QCM, other well established sensing platforms are commonly used as biosensors

* Corresponding authors at: Industrial Research Limited, Crown Research Institutes, 69 Gracefield Road, PO Box 31-310, Lower Hutt, New Zealand.
E-mail addresses: E.R.Hirst@massey.ac.nz (E.R. Hirst), Y.Yuan@irl.cri.nz (Y.J. Yuan).

0956-5663/$ – see front matter © 2008 Elsevier B.V. All rights reserved.
doi:10.1016/j.bios.2008.02.002

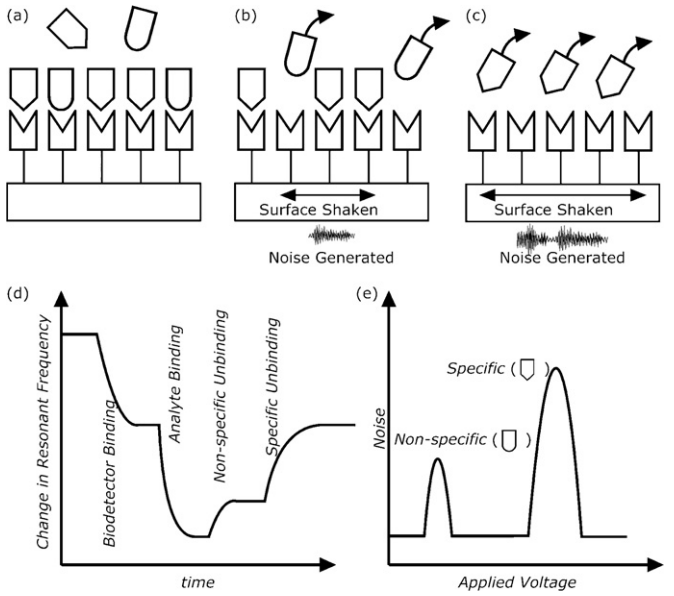

Fig. 1. Bond-rupture test concept. (a) Targets in the complex solution bind to the sensor surface forming both specific and non-specific bonds. (b) When the sensor surface is shaken at low amplitude, the non-specific bonds rupture and a small amount of noise is generated. (c) When the amplitude is increased to a suitably large the specifically bound targets will rupture and noise will be generated. (d) Concept resonant frequency results of bond-rupture test showing frequency change through the stages of preparation, binding and unbinding. (e) Concept noise results of bond-rupture test, the noise resulting from non-specific bond-rupture can be distinguished clearly. The height of the peaks is indicative of the amount of unbinding that has occurred.

including Surface Plasmon Resonance (SPR) (Hoa et al., 2007; Oh et al., 2004), potentiometric, capacitive (Berggren et al., 2001) biosensors and more (D'Orazio, 2003; Gizeli and Lowe, 1996; Jin-Woo et al., 1997; Luppa et al., 2001; Nakamura and Karube, 2003; Sokoll and Chan, 1999).

Acoustic wave sensors are also the subject of many papers and review articles (Chang et al., 2000; Grate and Frye, 1996; Drafts, 2001). Most applications of acoustic wave sensors as biosensors measure the properties of an attached mass, and are inherently plagued by the formation of non-specific bonds, i.e. where the attachment of non-target molecules, which are virtually indistinguishable from the attachment of target molecules because both the targeted and erroneous mass impact the measurand in the same way. Bond-rupture provides a means to detect the attached mass and distinguish between attachments of different affinity without costly and time-consuming labelling procedures. This technique has great potential for fast and accurate detection of disease and contamination at the point of care.

Fig. 1 shows the theory of operation of the bond-rupture sensor. The transducer surface is coated with receptors to which the target binds. Targets bind specifically and other molecules bind non-specifically (a). The surface is oscillated at increasing amplitude until bond-rupture occurs. By incrementing the force, particles of lower affinity rupture from the surface first (b), thus the additional mass caused by erroneous non-specific bonding is separated from the mass of interest which does not rupture until higher force (c). Fig. 1(d) and (e) shows some idealised resonant frequency results and noise results, respectively, from which the effects of specific and non-specific interactions can be differentiated. The height of the bond-rupture noise peaks Fig. 1(e) is a quantitative indicator of the number of bound ligands.

To date there have been a number of reported successful bond-rupture tests with varied results. Yuan et al. (2007) simultaneously measured the frequency change and noise signals from the rupture of microspheres bound to the QCM surface by biotin–streptavidin bonds. Cooper (2003) and Dultsev et al. (2000) both reported successful bond-rupture tests and successful noise capture with microspheres. In addition, the authors performed tests with biological targets (Cooper et al., 2001, Dultsev et al., 2001b). Edvardsson et al. (2005) attempted bond-rupture using a modified QCM-D instrument but failed to rupture the bonds. The QCM-D is a commercial surface science device commonly used for biosensing applications, e.g. (Hook et al., 1999).

2. Biological interface for bond-rupture sensor

The biodetector is critical to biosensor development, the problems with immobilisation are common to many biosensors and many researchers are participating in development. This section outlines important considerations that relate specifically to bond-rupture.

2.1. The significance of biological interactions

The bond-rupture experiments presented in the scientific literature have used a small sample of the receptors available. A common first step is the much studied and widely available biotin–streptavidin approximation (Dultsev et al., 2000; Yuan et al., 2007), a strong and stable specific bond which is easy to store and safe to use. Additionally bond-rupture tests have been performed on Maltose binding phage (Dultsev et al., 2001b), and the herpes simplex virus (Cooper, 2003; Cooper et al., 2001).

The underlying principle of the biodetector is to utilise specific recognition, the basis of enzyme–ligand interactions and antibody–antigen interactions. Non-covalent interactions such as hydrogen bonds and hydrophobic interactions produce molecular recognition, i.e. many weak interactions combine to form a strong, specific bond. Only when two molecules each possess topologically and chemically complimentary surfaces will the weak and localised interactions sum to an overall strong bond.

The bond-rupture technique requires specific attention to biodetector immobilisation, regeneration, affinity, and specificity. These characteristics are outlined with specific reference to generalised antibodies and aptamers in addition to the biotin–streptavidin bond that is a popular first step in biosensor development.

Biodetector affinity affects the rate of binding and overall strength of the bond. Bond-rupture requires a highly selective biodetector that maintains its selectivity in the presence of other specimen. High affinity allows the bond to be distinguished from its non-specific counterparts in a bond-rupture test. However if the affinity is too high, the bond may not rupture. The binding energy of specific bonds is ten times the amount of thermal energy at room temperature (k_BT) or more (Merkel, 2001).

Numerous immobilisation strategies have been used in many different applications and are the subject of a number of review articles, e.g. (Wink et al., 1997). For bond-rupture tests, the sensitive area, e.g. the QCM electrode, is coated with receptors. Gold is often favoured for the sensor surface because the direct attachment of recognition elements onto gold surfaces is well developed. Gold is chemically inert and used widely in piezoelectric, optical, and electrochemical sensors. Gold is used extensively – though not exclusively – in non-bond-rupture QCM sensor applications. Silver and platinum are also used.

Bond-rupture tests do not require regeneration procedures. Typical regeneration of the binding sites of antibodies requires stringent procedures. If a surrogate is available, bound particles

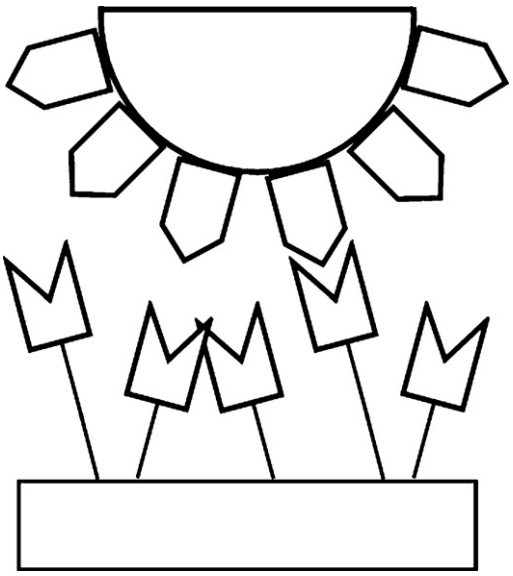

Fig. 2. Schematic example of random receptor orientation.

can be flushed away with a highly concentrated solution of related antigen with weak affinity. Regeneration using acid or alkaline solutions or ionic strength shock is potentially harmful to the receptor, leading insidious drift problems, and diminished life. To date there have been no reports of any quantitative studies into the effects bond-rupture has on the receptor.

2.2. Bond-rupture sensor receptor characteristics

Maintaining the specificity of the receptor is important for the measurement of analytes in all immuno-sensor systems. Immobilisation can cause some losses in the binding activity of some receptors (Wang et al., 2005), this loss in function has been associated with the random orientation of asymmetric molecules on the surface (Karyakin et al., 2000) as depicted in Fig. 2. It is desirable that the immobilisation preserves the native structure of the biomolecules, leaves the active sites accessible, and is exceptionally stable (Merkel, 2001). In general, directly adsorbed or screen printed enzymes and proteins lose sensitivity (Scouten et al., 1995).

Lack of stability is a problem for bioreceptors, but immobilisation has been shown to improve stability towards physical and chemical stress most of the time (Zoller and Smith, 1983). Out of 50 tested, 60% improved, 24% remained constant and 24% got worse. Additionally the sensitivity of an immuno-sensor was shown by Barie and Rapp (2001) to depend on the immobilisation method used. Usual immobilisation methods result in random orientation of biomolecules to the surface as depicted in Fig. 2. The immobilisation affects the specific binding constants because the apparent constants are dependant on the orientation of the biomolecule on the solid support. Direct adsorption gives no control over orientation and random orientation causes a distribution of the specific binding constants. Huang et al. (2004) found that only the rate of binding, and not the reverse reaction kinetics, is affected by the receptor orientation.

In addition to the effect on the receptor–ligand bond characteristics, the immobilisation method can directly influence the nature of the applied force during the bond-rupture test. The addition of intermediate layers with imperfect physical properties, significant thickness and inconsistent coverage change the absolute motion of the sensor surface and the bound particle. Ideal monolayers are perfectly aligned and closely packed, almost crystal like. The reality is that due to gold imperfections and the layer itself there are pin holes at a concentration of 1% of the area (Porter et al., 1987).

2.3. Receptors

There are many reviews and articles published about antibodies (Dall'Acqua and Carter, 1998) and aptamers, e.g. (Bunka and Stockley, 2006). Some key aspects of the receptors important to bond-rupture are outlined briefly below.

Immunoassays have utilised antibodies for decades and they are indispensable in most routine diagnostic tests. The antibody identification process starts within an animal, making antibody generation difficult for molecules that kill, e.g. toxins, or molecules that are inherently less immunogenic. Antibody identification is restricted to in vivo parameters; the identification of antibodies that can recognise targets outside physiological conditions is not feasible. Frozen stocks of antibody producing cells need to be stored at multiple sites to avoid accidental loss or death of cell lines. Antibodies have a limited shelf life and undergo irreversible denaturation when heated.

Aptamers, a relatively new and emerging technology offer a number of advantages over traditional antibodies (Tombelli et al., 2005). Aptamers, which range in size from 6 to 40 Da, can bond directly with the natural form of a protein, eliminating the need for linkers. Aptamers can be identified by in vitro selection – systematic evolution of ligands by exponential enrichment (SELEX) (Bunka and Stockley, 2006) – that does not depend on animal cells or physiological conditions. Aptamer selection is an automated process in contrast to the labour intensive and potentially costly antibody separation process. The in vitro selection conditions are manipulated to obtain aptamers with desirable properties, for example aptamers that bind to the target in a non-physiological buffer at non-physiological temperatures. Aptamers are stable to long-term storage, can be transported at ambient temperature and denaturation by heat is reversible within minutes. Additionally as aptamers are produced by chemical synthesis, the batch variations that require recalibrations are much less severe than receptors derived from live cells. The binding properties of aptamers can be selected based on the application. The rate of association and dissociation, affinity, and affinity to close molecules can be selected based on the intended application. An important consideration for point-of-care operation is that the procedures for using and storing aptamers are less stringent than for antibodies.

3. Transducer for bond-rupture sensor

The transducer converts the physical stimulus from the biodetector into an electric signal. Bond-rupture uses the piezoelectric effect to shake the sensor surface and convert the noise of bond-rupture into a detectable electrical signal. The Curie brothers, Pierre and Jacques in 1880, first observed piezoelectricity. Sauerbrey (1959) first used piezoelectric transducers as biosensors and worked toward the weighing of thin films adhered to the electrode surface of a QCM.

3.1. QCM, oscillation amplitude, and force

All reported bond-rupture results use QCM as the transducer. The properties of popular crystals and cuts are widely reported and published and commercial QCM devices are readily available. Most QCM biosensors measure changes to the resonant frequency and as such minimal variation of the measurand caused by variation in external stimulus, e.g. temperature, pressure, and humidity. When increasing the mass sensitivity of the device minute quantities of

attached surface mass are measured. This causes significant problems in liquid applications due to the susceptibility of the measured quantity to temperature, viscosity, and captured fluid. Material parameters such as the piezoelectric coupling coefficient and the dielectric constant are also important for achieving favourable sensor characteristics.

For bond-rupture sensors, the resonant frequency is measured so that the QCM can be driven at resonance to achieve the greatest displacement of the QCM. A number of approximations for QCM displacement have been used. The amplitude of the QCM displacement used by Cooper (2003) is

$$A = CQV_d \tag{1}$$

where $C = 1.4 \times 10^{-12}$ is a constant determined experimentally, Q the QCM merit factor (Q factor), and V_d is the driving voltage. The Q factor depends strongly on the viscosity reducing the QCM amplitude in liquid operation. This linear relationship was verified for V_d, ≤ 1 V, and has not been confirmed for higher voltages typical of bond-rupture scans (Borovsky et al., 2000).

Dultsev et al. (2000) used a power approximation where the amplitude is given by

$$A = \sqrt{\frac{QP}{2\pi^3 f^3 M}} \tag{2}$$

where P is the electrical power consumed by the QCM, and M is the effective mass of the QCM, considering that the amplitude is greater at the electrode center.

The QCM amplitude is at its highest at the centre of the electrode and vanishes at the edges, which was demonstrated experimentally and by modelling (Kurosawa et al., 2004). Experimental results are shown in Fig. 3. The resulting distribution is approximately Gaussian. The amplitude of QCM oscillations determined by

$$A(r) = A_{max}\, e^{-(r/c)^2} \tag{3}$$

where r is the distance from the electrode center and c is a Gaussian distribution coefficient determining the width of the curve (Edvardsson et al., 2005).

The operating frequency of the QCM influences the force applied on the bond. To increase the fundamental frequency of the QCM requires that the thickness be reduced making the device increasingly fragile. QCM can be operated at odd harmonics of the fundamental frequency, however Benes et al. (1995) showed that the electrode displacement, as illustrated in Fig. 3, is increasingly confined to the electrode centre as the order of harmonic is increased. The peak displacement at the center of the QCM is proportional to the inverse square of the harmonic order.

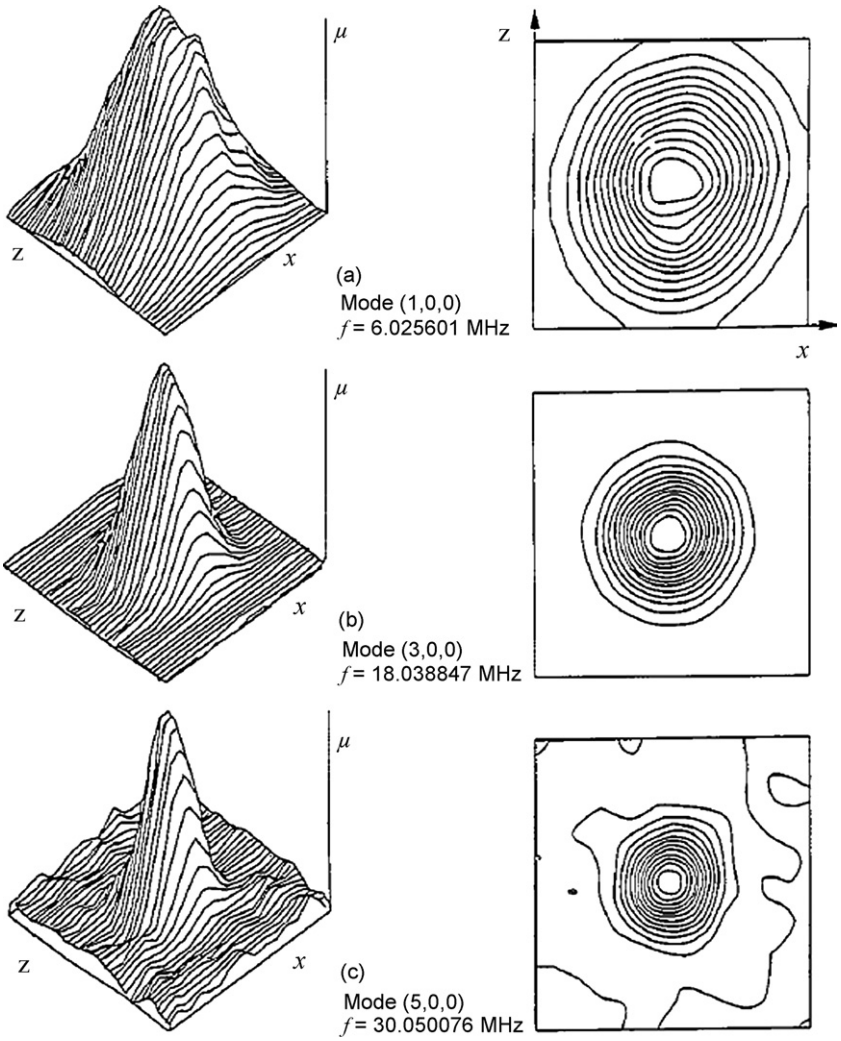

Fig. 3. Measured QCM spatial in-plane amplitude for (a) the fundamental mode, (b) the third harmonic, and (c) the fifth harmonic (Benes et al., 1995). Left column: three-dimensional representation of the shear vibration amplitude in arbitrary units. Right column: *iso*-amplitude line representation.

The force on the bond arises from the relative motion of the transducer surface and the attached particle. The acceleration of the particle and hence the force on the bond will depend on a variety of factors including the mass of the attached particle, its size and shape, and the nature of the bond. With a particle of appreciable size such as a microbead, thousands of bonds may form.

Cooper et al. (2001) presented a model for the force on the bond between the surface and a spherical particle. In reality, the analyte could be much smaller than a microbead and neither spherical, nor symmetrical. The particle is bound to a surface at a pivot point and assumed to be rolling about that point. Cooper's model predicts that the force on the bond is

$$F = \frac{2}{7} mA(2\pi f)^2 \tag{4}$$

where F is the force on bond (N), m the mass of particle (kg), A the maximum displacement or pivot point from centre position (m), and f is the frequency of surface oscillations (Hz). This model ignores any contribution of viscous forces, which would add additional drag to increase the force on the bond.

Sulfur–gold covalent bonds, utilised in some immobilisation methods, rupture at 1.4 nN under a 10 nN/s voltage ramp (Grandbois et al., 1999). This compares to 160 pN required for a single biotin–streptavidin bond indicating that the latter will rupture fires. Estimates indicate that approximately 10 μN of force is exerted on each sphere at rupture. Many bonds exist in parallel and the force generated is sufficient to rupture them.

If the QCM is operating in a flow cell and the fluid is moving, it will exert a force on the particle. Hydrodynamic techniques exploit this force when hydrodynamic drag exerts a small force on single bonds. Gaver and Kute (1998) modelled the forces on a cell adhered to the wall of a microchannel. The situation in a flow cell is analogous to the flow in a parallel wall chamber, where a bead, bound to the wall of a flow chamber is observed through a light microscope. Increased flow ruptures the bond and the bead is liberated (Merkel, 2001). Compared to the force from the oscillations and number of parallel bonds, the magnitude of the force resulting from flow will only be significant if the particles are large in relation to the channel width.

3.2. QCM and frequency change

The addition or removal of surface mass changes the resonant frequency of the QCM according to Sauerbrey (1959)

$$\Delta f = \frac{2f_0^2}{(\rho_q \mu_q)^{1/2}} \frac{\Delta m}{A} \tag{5}$$

where Δm is the increment of mass, A the area of the crystal, f_0 the resonant frequency, and ρ_q and μ_q are the density and shear modulus of the quartz respectively. This equation, called Sauerbrey's equation, only holds if the added mass is a uniform, thin, rigid film that couples perfectly to the crystal surface. Sauerbrey's equation is often abbreviated to

$$\Delta f = C_Q f^2 \frac{\Delta m}{A} \tag{6}$$

where C_Q is a constant.

In liquid, the change in frequency deviates from the linear model because of viscous losses due to soft films and liquid interaction and the effects of adsorbed water. When a rigid film is replaced by Newtonian bulk liquid the QCM resonant frequency shift is given by Kanazawa and Gordon (1985):

$$\Delta f = f_0^{3/2} \left(\frac{\eta_L \rho_L}{\pi \mu_Q \rho_Q} \right)^{1/2} \tag{7}$$

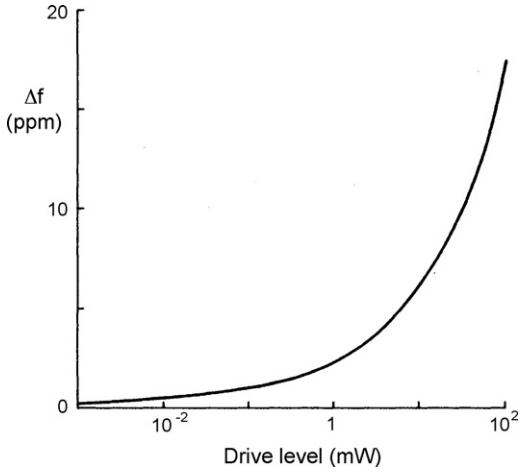

Fig. 4. Resonant frequency changing with diving power for an AT-cut device. At low powers the variation is attributed to the variation of elastic constants with strain. At higher powers heating effects are noticable (Brice, 1985).

where f_0 is the crystal frequency, η_L the liquid viscosity, ρ_L the liquid density, μ_Q the elastic modulus of the quartz, and ρ_Q is the density of the quartz.

This model is based on coupling of the shear wave in quartz to a damped shear wave in liquid. The total response of a rigid film immersed in liquid is a sum of film surface mass and the viscous contribution of the liquid. Voinova et al. (1997) showed by theoretical analysis that for non-rigid deposits the viscous loss of overlayers causes the deviation from Sauerbrey equation. The result is a reduction in the measured surface mass of the film

$$M_s = M(1 - \alpha) \tag{8}$$

where α is the viscous correction factor, which depends on the mechanical properties of the over-layer materials and viscous solution (η, ρ) and M is the true mass of the film. This predication is for the special case of pure viscous layers.

QCM biosensors and like timing crystals are predominantly manufactured from AT-cut quartz because the resonant frequency is stable at temperatures near the operating condition. Bond-rupture scans require that the power applied to the QCM is incrementally increased or ramped. The increased power in the QCM, through the interaction of temperature and other effects, changes with driving power. Experimental results such as those shown in Fig. 4 (Brice, 1985) are determined for driving powers that are lower than those used in bond-rupture scanning, but are indicative of the relationship and the severity of the effect.

The bond-rupture technique avoids all the problems associated with measuring only the resonant frequency by also detecting the noise generated by the bond-rupture event. Results of actual bond-rupture noise tests are shown in Fig. 5 (Dultsev et al., 2000). The results of specific receptor–ligand interaction being ruptured (1) and strong chemical bonds staying in tact (2) are shown as well as the results of a bond-rupture scan of weak physical bonds, which break at lower amplitude. The noise of bond-rupture on the vertical axes of Fig. 5 is measured in arbitrary units and the amplitude of the driving voltage is measured in Volts.

4. Electronic hardware for bond-rupture sensor

In order to achieve the maximum displacement the QCM is driven at resonance. There are two distinct approaches to achieve this, the first is to use the QCM as the frequency-determining element in an oscillator circuit, and the second is to detect the resonant

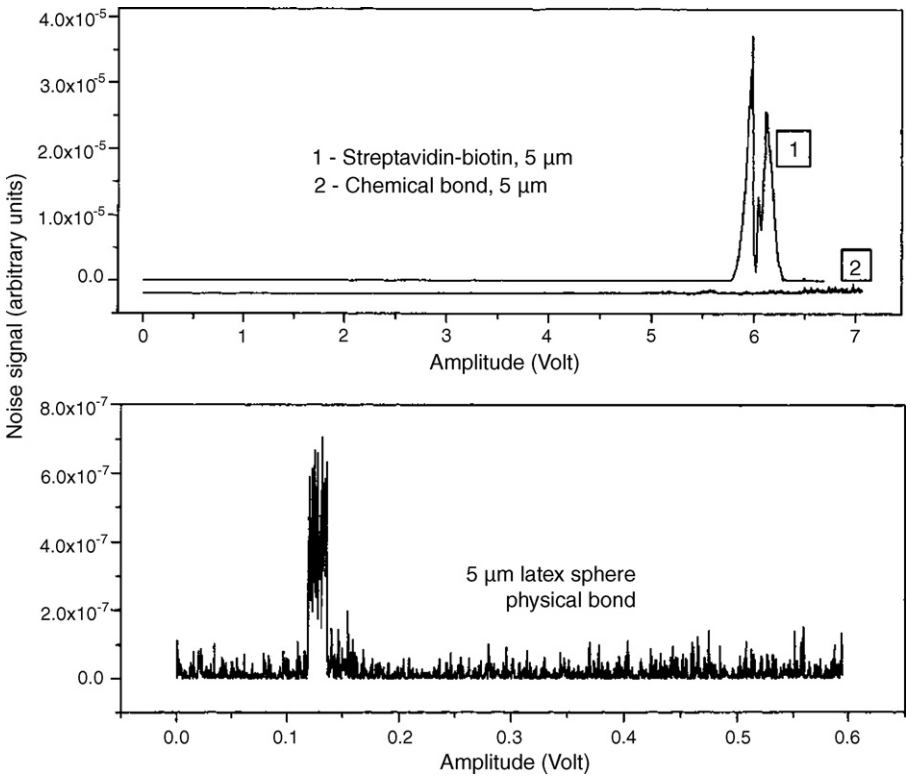

Fig. 5. Rupture force spectra of noise signal vs. applied voltage for a non-specific interaction (latex–gold), streptavidin–biotin interaction (streptavidin covalently attached to the latex sphere and biotinylated bovine serum albumin on the gold), and chemical bond (amide bond formed between an acid terminated thiol layer and an amine labelled latex sphere). All spheres are 5 μm in diameter (Dultsev et al., 2000).

frequency and feed this information to a sine wave source. The effect of mass change on the resonant frequency means that sine wave sources require closed loop feedback.

To minimise electrochemical interactions at the electrode surface the sensing electrode is grounded. The need to ramp the power makes oscillator circuits complex for bond-rupture implementation. QCM operation in liquids is now commonplace in biosensor applications. When operated in liquid, more sophisticated oscillators, such as that used by Borngraber et al. (2002), are required to compensate for heavy damping. Changes in the resonant frequency can be detected using high-speed counters or other circuits. There are many articles addressing oscillators for mass balance applications only some of which are listed here: Arnau et al. (2002), Auge et al. (1995), Eichelbaum et al. (1999), Ehahoun et al. (2002), Ferrari et al. (2000, 2001) and Schroder et al. (2002).

Of particular interest in bond-rupture sensors is the detection of the noise of bond-rupture. Detachment events are not entirely random since they occur near the maxima of acceleration and displacement (Dultsev et al., 2000). The resulting noise signal of interest is broadband with peaks near the fundamental frequency and its harmonics. The QCM is a one-port device, thus small signals of interest like the noise of bond-rupture are superimposed on top of the driving signal. If the signal of interest were in the same frequency range as the driving signal, it would be impossible to separate two. The noise of bond-rupture is detected by focusing on a frequency band that is not occupied by the driving signal or its artefacts, filtering can be achieved in hardware or software.

Dultsev et al. (2000) and Cooper et al. (2001) used a network of separate instruments controlled by a computer to drive the QCM at its fundamental, and monitor the noise at the third harmonic. This is shown in Fig. 6(a). Both authors used a phase locked loop to monitor the noise generated by bond-rupture. The former detected

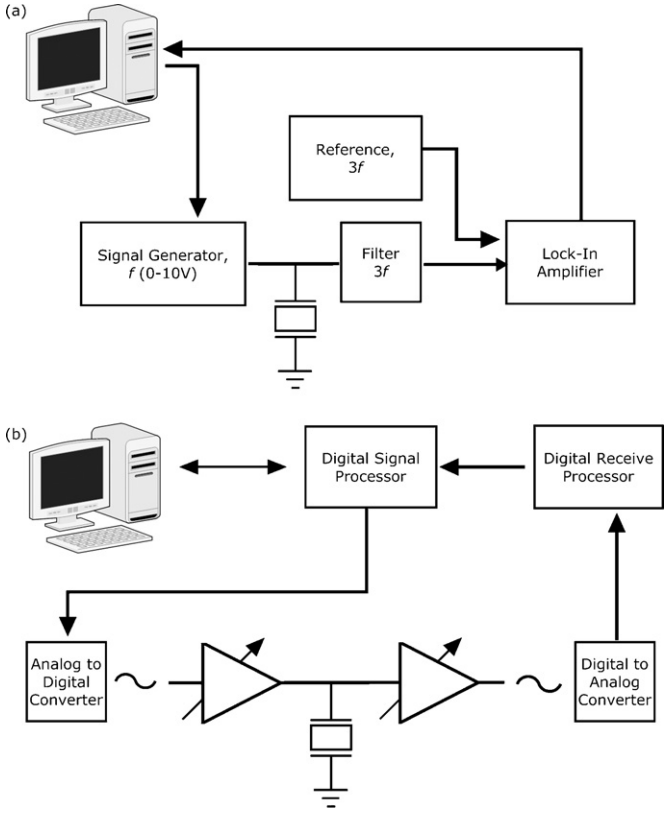

Fig. 6. (a) Diagram of instrumentation approach for bond-rupture noise test used by Cooper (2003), Cooper et al. (2001) and Dultsev et al. (2000, 2001b) and (b) diagram of integrated digital approach for bond-rupture testing used by van der Werff et al. (2007).

noise at a frequency close to, but not exactly, the third harmonic ($3F + \Delta f$), where Δf was 85 kHz, and the latter detected noise at three times the fundamental.

A more integrated digital approach (Fig. 6(b)) was employed by van der Werff et al. (2007) and Yuan et al. (2007), where the resonant frequency of the QCM was determined by sweeping through frequencies near resonance and monitoring the peak voltage across the QCM. This requires discontinuity in the driving signal, which is stopped periodically to re-test the resonant frequency. The use of specifically designed circuit boards in the place of expensive discrete devices brings bond-rupture devices closer to the point-of-care.

Edvardsson et al. (2005), using a modified QCM-D instrument, drove the crystal in a similar manner, oscillating the QCM at the fundamental for the monitoring of dissipation and resonant frequency, and further driving at a higher harmonic in order to influence binding. Driving at the third harmonic, they were unable to induce bond-rupture. The authors attributed this to insufficient crystal oscillation amplitude, decreased torque due to virus shape, and stronger antibody–antigen binding.

5. Modelling forced bond rupture

Forced bond-rupture is performed in various experimental platforms. Weak non-covalent interactions such as antibody–antigen bonds have limited lifetimes and so will dissociate under almost any level of force if pulled for modest periods. Close to equilibrium in solution large numbers of molecules continuously bond and dissociate under zero force (Evans, 2001). Such studies are focused on the study of single bonds but still offer some insight into the principles of bond-rupture.

Bond strength is usually tested using an AFM, where the microcantilever apparatus strains the bond vertically until breakage, e.g. (Janshoff and Steinem, 2001a). Other methods include parallel wall flow chamber, bead doublet in shear flow, and magnetic force breakage, Merkel (2001) detailed these methods. The force required to induce bond dissociation falls in the range from 2 to 200 pN.

A number of articles offer mathematical descriptions of single bond-rupture: (Merkel et al., 1999; Merkel, 2001; Evans et al., 1995; Evans and Ritchie, 1997, 1999; Evans, 1998, 2001; Raible et al., 2004), all of which address the rupture of single, or few, bonds. In force spectroscopy experiments, the effect of an applied force on the dissociation rate $k_{off}(f)$ is considered, and many approximations are offered by the literature. Following Evans and Ritchie (1997) a rupture event is viewed as a thermally activated decay of a metastable state governed by reaction kinetics of the form

$$\frac{dp(t)}{dt} = -k_{off}(f(t))p(t) \quad (9)$$

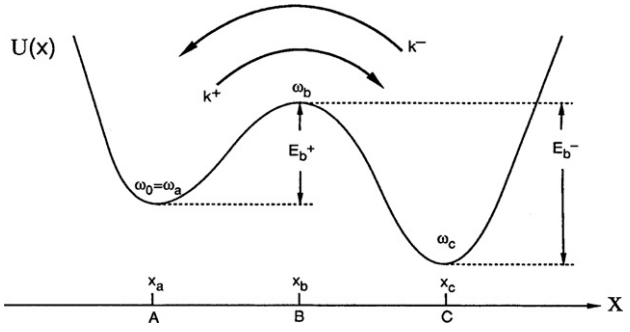

Fig. 7. A simple model of reaction kinetics (Hanggi et al., 1990).

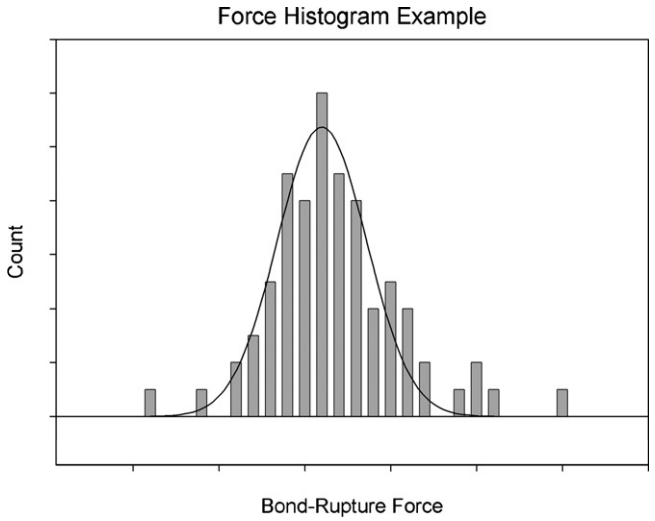

Fig. 8. Force histograms indicating distributions of bond-rupture force.

where $p(t)$ is the probability of bond survival up to time, t, and $k_{off}(f)$ is the rate of decay in the presence of a force, f. Implicit in the above assumption is that the probability of bond-rupture only depends on the instantaneously acting force and not on the history.

To all practical purposes the forced rupture of a bond results in infinite separation resulting in virtually no chance of bond reformation, thus the bond reformation is exponentially suppressed and therefore neglected.

An external force lowers the barrier in the energy landscape (E_b) and bond lifetime shortens. Fig. 7 shows the assumed form of reaction kinetics. The figure assumes confinement by a single barrier, which is seldom the case. The energy path goes from one deep minimum over a saddle point into another deep minimum and is bound by steeply rising energy in other directions. Multiple reaction pathways are handled to some extent by Raible et al. (2004) who introduced a second meta stable bound state with different kinetics.

Bond strength, typically thought of as the force at which the bond breaks, is amended to the force at which the bond is most likely to break, i.e. the peak of the distribution of rupture forces in Fig. 8. This distribution of forces means that the many bonds anchoring one particle may not rupture at the same time, and likewise particles on a single transducer are not liberated simultaneously.

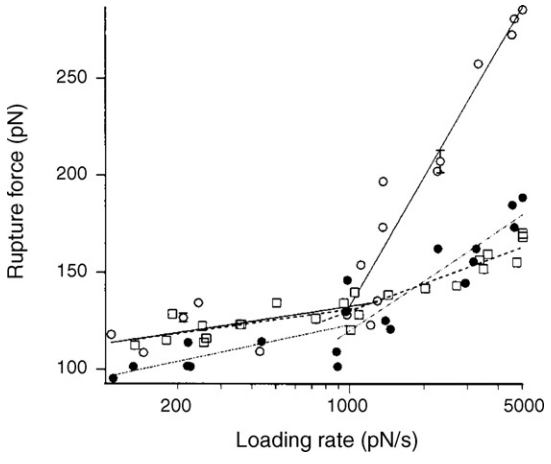

Fig. 9. Rupture force depends on loading rate (Yuan et al., 2000).

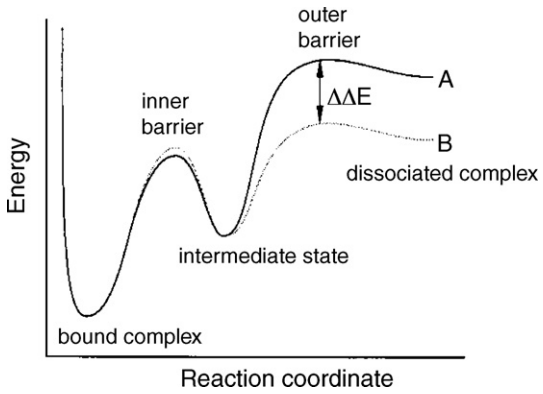

Fig. 10. Conceptual landscape of biotin–streptavidin interactions (Yuan et al., 2000).

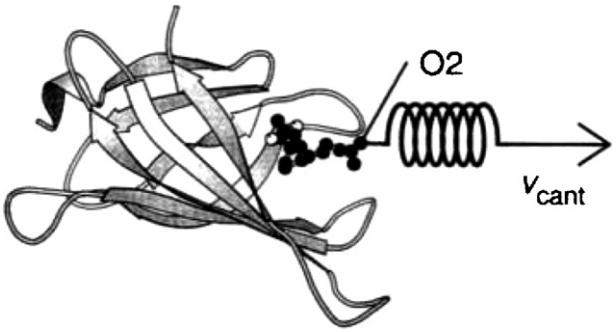

Fig. 11. Ribbon model for computer simulation of biotin–streptavidin separation (Grubmuller et al., 1996).

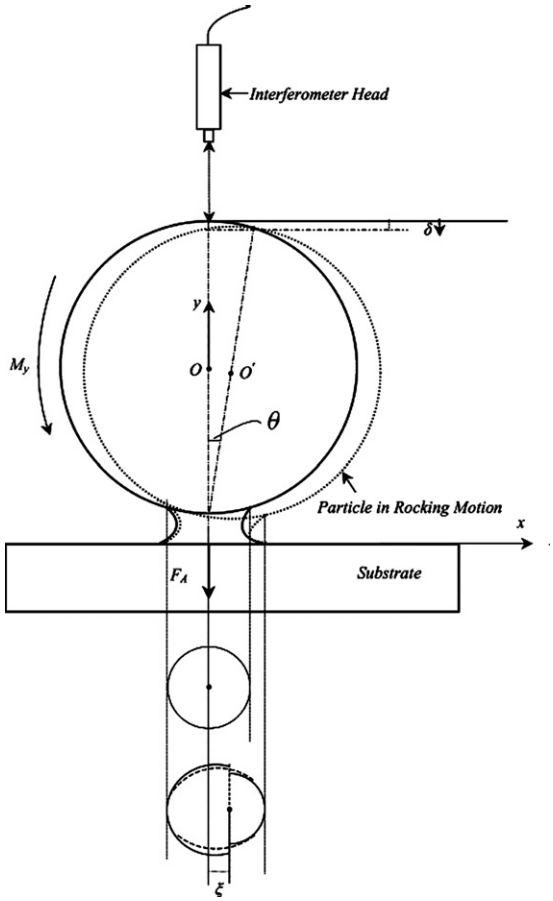

Fig. 12. Rocking motion of a particle subjected to base excitation (Peri and Cetinkaya, 2005).

The location of the force peak moves depending on the rate at which the load is applied (Lo et al., 2001; Yuan et al., 2000). Fig. 9 shows experimental results that indicate that the rupture force scales linearly with the logarithm of the loading rate, and that for biotin–streptavidin bonds two such schemes exist. This is indicative of reaction kinetics as shown in Fig. 10. When the loading rate is low there is an increased chance that bond breakage will occur due to thermal fluctuations while there is still a barrier to bond breakage (Dultsev et al., 2000). Essentially, when the loading rate is low, more time is spent with low force applied. This increases the likelihood that the bond will break at the low force.

The rupture of single ligand–receptor bonds has been modelled using molecular mechanics such as Grubmuller et al. (1996), Heymann and Grubmuller (2001) and Stayton et al. (1999), the applied force in the model was designed to mimic an AFM experiment (Fig. 11).

A technique analogous to QCM bond-rupture has been used to study adhesion of solids and liquids, where a particle is shaken by an ultrasound transducer and its motion is studied by laser interferometery (Fig. 12) (Peri and Cetinkaya, 2005). The authors did not apply this technique to bond-rupture but used it to study the properties of a non-biologically derived adhesion layer.

An important consideration when comparing models is the direction and nature of the force. AFM bond strength experiments are conducted on single bonds using a continuous force applied in one direction, this is in contrast to QCM studies where the force is oscillatory. The force distribution between all the bonds attached to a single particle will be uneven and time varying. That is, the bonds on the outside of a rocking particle will be under more strain than those nearer the centre. The complex shapes will create torques and unsymmetrical contact areas that will only serve to widen the distribution of measured bond forces.

6. Discussion

Bond-rupture biosensors are still a way away from the easy-to-use, point-of-care magic wand that is the goal of most biosensor researchers. Operation in complex solutions with small lot-lot variations, high analytical sensitivity, and low interference has not been reported. There are a number of promising avenues for research in this field.

One such opportunity is the implementation of bond-rupture on other acoustic wave devices, or using combinations of two or more devices. There are many acoustic wave devices that could potentially be applied to bond-rupture, including, but not limited to flexural plate wave (FPW) devices, micro-electro-mechanical systems (MEMS) devices such as cantilevers and a multitude of different SAW configurations (Grate and Frye, 1996; Chang et al., 2000; Drafts, 2001; Hauptmann et al., 2003; Janshoff et al., 2000; Du et al., 1996; Lange et al., 2003).

It has been suggested that two or more transducers can be incorporated into one sensor. For SAW devices, multiple transducers could be used to detect the noise in different frequency bands or propagation direction (Dultsev et al., 2001a). Separate ultrasonic transducers, i.e. not constructed on the same crystal as the receiving transducer, could be used to cause rupture and SPR for rupture detection (Yuan et al., 2005).

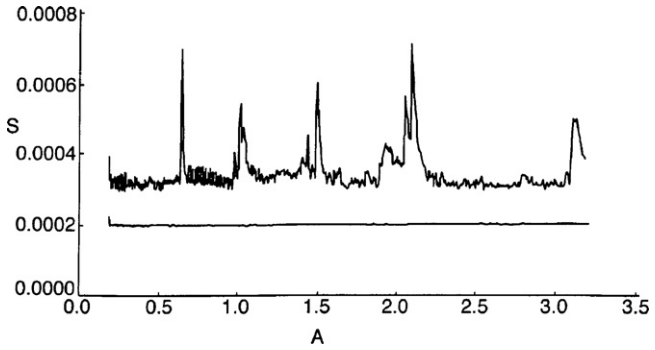

Fig. 13. Sample of bond-rupture of physical bonds captured using a SAW device (Dultsev et al., 2001a).

The principle of SAW bond-rupture is much the same for as QCM, however there are distinct differences that indicate that SAW devices provide much promise for this platform. The principle of SAW bond-rupture has been confirmed in a patent by Dultsev et al. (2001a). The results, shown in Fig. 13, are less consistent than QCM as less work has been done on the SAW platform. The vertical axis measures bond-rupture noise in S (arbitrary units) and the driving amplitude is measured in volts.

SAW devices, while exhibiting less displacement can be operated at high frequency without thinning the substrate and making the device more fragile. In addition, SAW electrodes are located on the same side of the device. In acoustic plate mode (APM) devices, the opposite side can be used as the sensor simplifying flow cell integration and wiring. SAW devices can be probed wirelessly (Freudenberg et al., 1999) meaning that many such devices can be switched easily. Alternatively wireless probing of QCM has been achieved (Ogi et al., 2006a,b; Thompson et al., 2003). In this mode of operation, the electrodes of the QCM are lighter than is otherwise possible in wired QCM, and the antenna are positioned on one side of the QCM.

Inter-Digitated Electrodes (IDTs) generate surface acoustic waves. Specific frequency characteristics of the IDT can incorporate passive signal processing into the device itself. SAW are manufactured using conventional IC microfabrication techniques, even CMOS processes (Tigli and Zaghloul, 2007). This means active signal processing could also be incorporated into the sensor device.

A core concern with SAW bond-rupture will be the ability of the device to withstand the high powers required to cause bond-rupture. Pekarcikova et al. (2005) showed the effect of high power in SAW electrode structures. Metal migration (Fig. 14) can cause shorts or discontinuities, reduction in device life and drift problems.

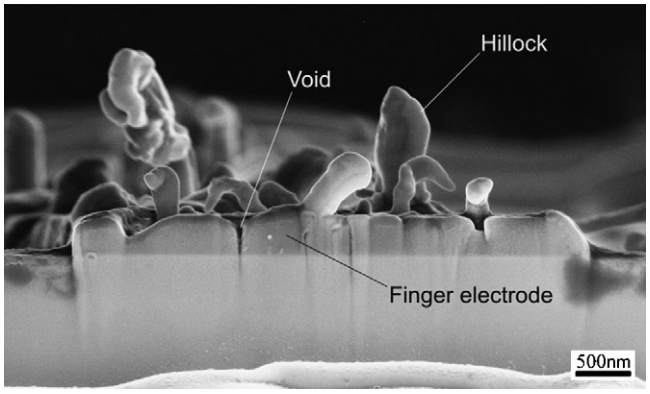

Fig. 14. SEM/SE image of a cross section of an Al finger electrode after loading with 3 W for 2000 min (Pekarcikova et al., 2005).

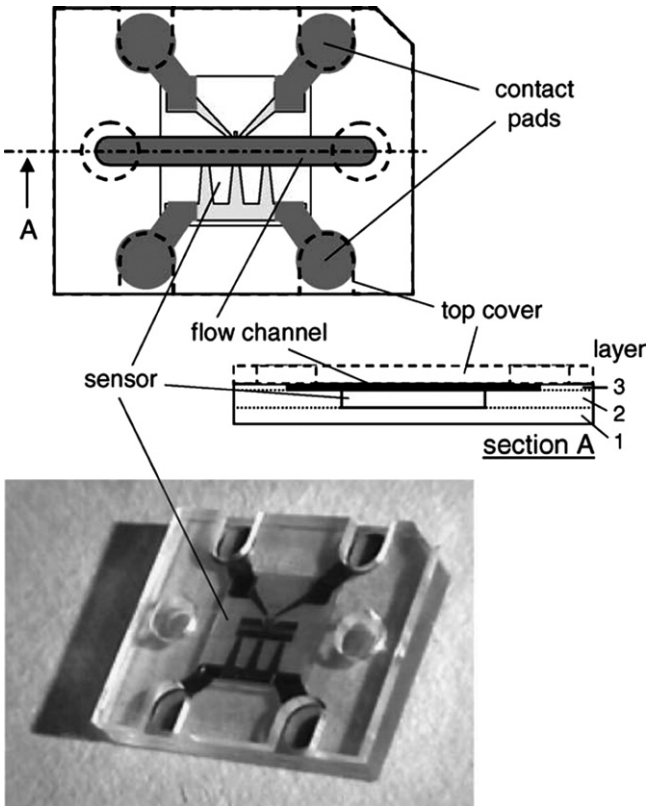

Fig. 15. Encapsulated SAW biosensor, 8 mm × 10 mm (Lange et al., 2006).

Flow cell integration of a SAW device such as that shown in Fig. 15 can achieve very low volumes. To alleviate pressure on the piezoelectric substrate capacitive coupling is used (Lange et al., 2006). Bond-rupture would be good platform for integration into complex 'lab on a chip' type devices, and there is potential for the integration of SAW and QCM devices with complex electronics. There are many examples of applications where SAW and QCM have been utilised in such systems (Ghafar-Zadeh et al., 2007; Beeley et al., 2004; Garcia et al., 2006; Lange et al., 2006; Hierlemann et al., 2003).

There are a number of theoretical avenues for research. None of the existing models and results for single bond spectroscopy or adhesion layers outlined above is a perfect fit for what occurs in a bond-rupture test. The dynamics of bond-rupture are not well known, and a greater understanding is needed.

Integration and automation with electronics and flow cells could reduce costs of the device and increase throughput.

7. Conclusion

Bond-rupture biosensors have the potential to deliver the state-of-the-art in clinical testing and contaminant detection technology to the point-of-care. Affirmative diagnosis of a specifically threatening disease or contamination and even quantitative determination of the concentration could be achieved with a turnaround time of less than 1 h.

Real-world biosensors are required to detect low concentrations of the analyte in the presence of many interfering phenomena. Bond-rupture, unlike pure mass-balance architectures could work

in complex serum, e.g. blood, separating the effect of non-specific binding. Like many biosensors, the application of the bond-rupture technique depends directly on the existence or development of a suitably viable receptor.

This review has explored current progress in developing this platform and outlines some future prospects including the use of other acoustic wave devices, circuit integration and smart sensing, and microfluidic cell integration.

Acknowledgements

This work was performed under the auspices of the Foundation for Research, Science and Technology of New Zealand by Industrial Research Ltd. under New Economy Research Fund C08X0408 to Y.J. Yuan. Thanks are given to M.J. van der Werff for numerous valuable discussions.

References

Arnau, A., Sogorb, T., Jimenez, Y., 2002. Rev. Sci. Instrum. 73, 2737.
Auge, J., Hauptmann, P., Hartmann, J., Rosler, S., Lucklum, R., 1995. Sens. Actuators B: Chem. 24, 43–48.
Barie, N., Rapp, M., 2001. Biosens. Bioelectron. 16, 979–987.
Beeley, J.M., Mills, C., Hammond, P.A., Glidle, A., Cooper, J.M., Wang, L., Cumming, D.R.S., 2004. Sens. Actuators B: Chem. 103, 31–36.
Benes, E., Groschl, M., Burger, W., Schmid, M., 1995. Sens. Actuators A: Phys. 48, 1–21.
Berggren, C., Bjarnason, B., Johansson, G., 2001. Electroanalysis 13, 173–180.
Borngraber, R., Schroder, J., Lucklum, R., Hauptmann, P., 2002. IEEE Trans. Ultrason. Ferroelectr. Freq. Control 49, 1254–1259.
Borovsky, B., Mason, B.L., Krim, J., 2000. J. Appl. Phys. 88, 4017–4021.
Brice, J.C., 1985. Rev. Modern Phys. 57, 105 LP - 146.
Bunka, D.H.J., Stockley, P.G., 2006. Nat. Rev. Microbiol. 4, 588–596.
Chang, S.M., Muramatsu, H., Nakamura, C., Miyake, J., 2000. Mater. Sci. Eng. C: Biomimetic Supramol. Syst. 12, 111–123.
Cooper, M.A., 2003. Meas. Sci. Technol. 14, 1888–1893.
Cooper, M.A., Singleton, V.T., 2007. J. Mol. Recognit. 20, 154–184.
Cooper, M.A., Dultsev, F.N., Minson, T., Ostanin, V.P., Abell, C., Klenerman, D., 2001. Nat. Biotechnol. 19, 833–837.
Dall'Acqua, W., Carter, P., 1998. Curr. Opin. Struct. Biol. 8, 443–450.
D'Orazio, P., 2003. Clin. Chim. Acta 334, 41–69.
Drafts, B., 2001. IEEE Trans. Microwave Theory Tech. 49, 795–802.
Du, J., Harding, G.L., Ogilvy, J.A., Dencher, P.R., Lake, M., 1996. Sens. Actuators A: Phys. 56, 211–219.
Dultsev, F.N., Ostanin, V.P., Klenerman, D., 2000. Langmuir 16, 5036–5040.
Dultsev, F.N., Klenerman, D. Ostanin, V.P., 2001. WO2000GB01587 20000425 11-01-2001.
Dultsev, F.N., Speight, R.E., Florini, M.T., Blackburn, J.M., Abell, C., Ostanin, V.P., Klenerman, D., 2001b. Anal. Chem. 73, 3935–3939.
Edvardsson, M., Rodahl, M., Kasemo, B., Hook, F., 2005. Anal. Chem. 77, 4918–4926.
Ehahoun, H., Gabrielli, C., Keddam, M., Perrot, H., Rousseau, P., 2002. Anal. Chem. 74, 1119-+.
Eichelbaum, F., Borngraber, R., Schroder, J., Lucklum, R., Hauptmann, P., 1999. Rev. Sci. Instrum. 70, 2537–2545.
Evans, E., 1998. Faraday Discuss., 1–16.
Evans, E., 2001. Annu. Rev. Biophys. Biomol. Struct. 30, 105–128.
Evans, E., Ritchie, K., 1997. Biophys. J. 72, 1541–1555.
Evans, E., Ritchie, K., 1999. Biophys. J. 76, 2439–2447.
Evans, E., Ritchie, K., Merkel, R., 1995. Biophys. J. 68, 2580–2587.
Ferrari, V., Marioli, D., Taroni, A., 2000. Electron. Lett. 36, 610–612.
Ferrari, V., Marioli, D., Taroni, A., 2001. IEEE Trans. Instrum. Meas. 50, 1119–1122.
Freudenberg, J., Schelle, S., Beck, K., Von Schickfus, M., Hunklinger, S., 1999. Biosens. Bioelectron. 14, 423–425.
Garcia, M., Fernandez, M.J., Fontecha, J.L., Lozano, J., Santos, J.P., Aleixandre, M., Sayago, I., Gutierrez, J., Horrillo, M.C., 2006. Talanta 68, 1162–1165.
Gaver, D.P., Kute, S.M., 1998. Biophys. J. 75, 721–733.
Ghafar-Zadeh, E., Sawan, M., Therriault, D., 2007. Sens. Actuators A: Phys. 134, 27–36.
Gizeli, E., Lowe, C.R., 1996. Curr. Opin. Biotechnol. 7, 66–71.
Godber, B., Thompson, K.S.J., Rehak, M., Uludag, Y., Kelling, S., Sleptsov, A., Frogley, M., Wiehler, K., Whalen, C., Cooper, M.A., 2005. Clin. Chem. 51, 1962–1972.
Grandbois, M., Beyer, M., Rief, M., Clausen-Schaumann, H., Gaub, H.E., 1999. Science 283, 1727–1730.
Grate, J.W., Frye, G.C., 1996. Sens. Update 2, 37–83.
Grubmuller, H., Heymann, B., Tavan, P., 1996. Science 271, 997–999.
Hanggi, P., Talkner, P., Borkovec, M., 1990. Rev. Modern Phys. 62, 251–341.
Hauptmann, P., Lucklum, R., Schroder, J., 2003. Proceedings of the IEEE Symposium on Ultrasonics.
Heymann, B., Grubmuller, H., 2001. Biophys. J. 81, 1295–1313.
Hierlemann, A., Brand, O., Hagleitner, C., Baltes, H., 2003. Proceedings of the IEEE 91. 839–863.
Hoa, X.D., Kirk, A.G., Tabrizian, M., 2007. Biosens. Bioelectron. 23, 151–160.
Hook, F., Rodahl, M., Keller, C., Glasmastar, K., Fredriksson, C., Dahiqvist, P., Kasemo, B., 1999. Proceedings of the 1999 Joint Meeting of the European Frequency and Time Forum, 1999 and the IEEE International Frequency Control Symposium.
Huang, L., Cooper, M.A., 2006. Clin. Chem. 52, 2148–2151.
Huang, J., Chen, J., Chesla, S.E., Yago, T., Mehta, P., Mcever, R.P., Zhu, C., Long, M., 2004. J. Biol. Chem. 279, 44915–44923.
Janshoff, A., Steinem, C., 2001a. Chemphyschem 2, 577–579.
Janshoff, A., Steinem, C., 2001b. Sens. Update 9, 313–354.
Janshoff, A., Galla, H.J., Steinem, C., 2000. Angew. Chem. Int. Ed. 39, 4004–4032.
Jin-Woo, C., Ying, D., Ahn, C.H., Halsall, H.B., Heineman, W.R., 1997. Proceedings of the 19th International Conference IEEE/EMBS, Chicago, IL, USA.
Kanazawa, K.K., Gordon, J.G., 1985. Anal. Chem. 57, 1770–1771.
Karyakin, A.A., Presnova, G.V., Rubtsova, M.Y., Egorov, A.M., 2000. Anal. Chem. 72, 3801–3811.
Kurosawa, S., Aizawa, H., Tozuka, M., Nakamura, M., Park, J.W., 2003. Meas. Sci. Technol. 14, 1882–1887.
Kurosawa, C., Kurosawa, S., Aizawa, H., Horibe, T., 2004. Proceedings of the 2004 IEEE International Frequency Control Symposium and Exposition.
Lange, K., Bender, F., Voigt, A., Gao, H., Rapp, M., 2003. Anal. Chem. 75, 5561–5566.
Lange, K., Blaess, G., Voigt, A., Gotzen, R., Rapp, M., 2006. Biosens. Bioelectron. 22, 227–232.
Lo, Y.S., Zhu, Y.J., Beebe, T.P., 2001. Langmuir 17, 3741–3748.
Luppa, P.B., Sokoll, L.J., Chan, D.W., 2001. Clin. Chim. Acta 314, 1–26.
Merkel, R., 2001. Phys. Rep. Rev. Phys. Lett. 346, 344–385.
Merkel, R., Nassoy, P., Leung, A., Ritchie, K., Evans, E., 1999. Nature 397, 50–53.
Nakamura, H., Karube, I., 2003. Anal. Bioanal. Chem. 377 (October 3), 446–468, SO.
Ogi, H., Motohisa, K., Matsumoto, T., Mizugaki, T., Hirao, M., 2006a. Biosens. Bioelectron. 21, 2001–2005.
Ogi, H., Motoshisa, K., Matsumoto, T., Hatanaka, K., Hirao, M., 2006b. Anal. Chem. 78, 6903–6909.
Oh, B.K., Kim, Y.K., Park, K.W., Lee, W.H., Choi, J.W., 2004. Biosens. Bioelectron. 19, 1497–1504.
Pekarcikova, M., Hofmann, M., Menzel, S., Schmidt, H., Gemming, T., Wetzig, K., 2005. IEEE Trans. Ultrason. Ferroelectr. Freq. Control 52, 911–917.
Peri, M.D.M., Cetinkaya, C., 2005. J. Colloid Interf. Sci. 288, 432–443.
Porter, M.D., Bright, T.B., Allara, D.L., Chidsey, C.E.D., 1987. J. Am. Chem. Soc. 109, 3559–3568.
Raible, M., Evstigneev, M., Reimann, P., Bartels, F.W., Ros, R., 2004. J. Biotechnol. 112, 13–23.
Sauerbrey, G., 1959. Z. Phys. 155, 206–222.
Schroder, J., Borngraber, R., Eichelbaum, F., Hauptmann, P., 2002. Sens. Actuators A: Phys. 97-8, 543–547.
Scouten, W.H., Luong, J.H.T., Stephen Brown, R., 1995. Trends Biotechnol. 13, 178–185.
Sokoll, L.J., Chan, D.W., 1999. Anal. Chem. 71, 356R–362R.
Stayton, P.S., Freitag, S., Klumb, L.A., Chilkoti, A., Chu, V., Penzotti, J.E., To, R., Hyre, D., Le Trong, I., Lybrand, T.P., Stenkamp, R.E., 1999. Biomol. Eng. 16, 39–44.
Thompson, M., Ballantyne, S.M., Cheran, L.E., Stevenson, A.C., Lowe, C.R., 2003. Analyst 128, 1048–1055.
Tigli, O., Zaghloul, M.E., 2007. IEEE Sens. J. 7, 219–227.
Tombelli, S., Minunni, M., Luzi, E., Mascini, M., 2005. Bioelectrochemistry 67, 135–141.
Van Der Werff, M.J., Yuan, Y.J., Hirst, E.R., Xu, W.L., Chen, H., Bronlund, J.E., 2007. Sens. J. IEEE 7, 762–769.
Voinova, M.V., Jonson, M., Kasemo, B., 1997. J. Phys. Condens. Matter 9, 7799–7808.
Wang, H., Wu, J., Li, J.S., Ding, Y.J., Shen, G.L., Yu, R.Q., 2005. Biosens. Bioelectron. 20, 2210–2217.
Wink, T., Zuilen, S.J.V., Bult, A., Bennekom, W.P.V., 1997. Analyst 122, 43–50.
Yuan, C., Chen, A., Kolb, P., Moy, V.T., 2000. Biochemistry 39, 10219–10223.
Yuan, Y., Andrews, M., Arnold, M.W., Marlow, B., 2005. PCT/NZ2005/000051 March 19, 2004.
Yuan, Y.J., Van Der Werff, M.J., Chen, H., Hirst, E.R., Xu, W.L., Bronlund, J.E., 2007. Anal. Chem. 79, 9039–9044.
Zoller, M.J., Smith, M., 1983. Methods Enzymol. 100, 468–500.